Shigella flexneri Regulation of ARF6 Activation during Bacterial Entry via an IpgD-Mediated Positive Feedback Loop

RESEARCH ARTICLE

Shigella flexneri Regulation of ARF6 Activation during Bacterial Entry via an IpgD-Mediated Positive Feedback Loop

Anna Cristina Garza-Mayers,[a] Kelly A. Miller,[b] Brian C. Russo,[b] Dipal V. Nagda,[b]* Marcia B. Goldberg[a,b]

Department of Microbiology and Immunobiology, Harvard Medical School, Boston, Massachusetts, USA[a]; Department of Medicine, Division of Infectious Diseases, Massachusetts General Hospital, Cambridge, Massachusetts, USA[b]

* Present address: Dipal V. Nagda, Brown University, Providence, Rhode Island, USA

ABSTRACT **Entry into cells is critical for virulence of the human bacterial pathogens *Shigella* spp. *Shigella* spp. induce membrane ruffle formation and macropinocytic uptake, but the events instigating this process are incompletely understood. The host small GTPase ADP-ribosylation factor 6 (ARF6) functions in membrane trafficking at the plasma membrane and activates membrane ruffle formation. We demonstrate that ARF6 is required for efficient *Shigella flexneri* entry, is activated by *S. flexneri* dependent on the phosphatase activity of the type III secreted effector IpgD, and depends on cytohesin guanine nucleotide exchange factors (GEFs) for recruitment to entry sites. The cytohesin GEF ARF nucleotide binding site opener (ARNO) is recruited to these sites, also dependent on IpgD phosphatase activity. ARNO recruitment is independent of ARF6, indicating that, in addition to the described recruitment of ARNO by ARF6, ARNO is recruited upstream of ARF6. Our data provide evidence that ARF6, IpgD, phosphoinositide species, and ARNO constitute a previously undescribed positive feedback loop that amplifies ARF6 activation at bacterial entry sites, thereby promoting efficient *S. flexneri* uptake.**

IMPORTANCE ***Shigella* spp. cause diarrhea and dysentery by infection of epithelial cells in the human colon. Critical to disease is the ability of *Shigella* to enter into cells, yet the mechanisms involved in entry are incompletely understood. We demonstrate that the small GTPase ADP-ribosylation factor 6 (ARF6) is required for efficient cellular entry of *Shigella flexneri* and that activation of ARF6 depends on the phosphatase activity of the *Shigella* protein IpgD, which is introduced into cells via the bacterial type III secretion system. We further show that IpgD phosphatase activity is required for recruitment of the ARF6 guanine nucleotide exchange factor (GEF) ARF nucleotide binding site opener (ARNO) to bacterial entry sites and that ARNO lies upstream of ARF6 activation. These relationships define a positive feedback loop that contributes to activation of ARF6 at *S. flexneri* entry sites and leads to local amplification of signals that promote bacterial entry.**

Received 30 December 2014 **Accepted** 13 January 2015 **Published** 3 March 2015

Citation Garza-Mayers AC, Miller KA, Russo BC, Nagda DV, Goldberg MB. 2015. *Shigella flexneri* regulation of ARF6 activation during bacterial entry via an IpgD-mediated positive feedback loop. mBio 6(2):e2584-14. doi:10.1128/mBio.02584-14.

Editor Jeff F. Miller, UCLA School of Medicine

Address correspondence to Marcia B. Goldberg, marcia.goldberg@mgh.harvard.edu.

This article is a direct contribution from a Fellow of the American Academy of Microbiology.

Shigella spp. are Gram-negative bacterial pathogens that cause diarrheal disease by invading and spreading through the colonic epithelium. *Shigella* entry into intestinal epithelial cells is critical to the disease process (1, 2) and requires a type III secretion system (T3SS) and secreted effectors (2, 3). Upon contact with nonphagocytic cells, delivery of T3SS effector proteins causes rearrangements of the actin cytoskeleton, which induce plasma membrane ruffling that leads to macropinocytic uptake of the pathogen (4).

Several bacterial and host proteins have been shown to be involved in *Shigella* entry. Disruption of the activity of individual proteins leads to defects but not to complete abrogation of entry, indicating that entry pathways are partially redundant. *Shigella* IpaA promotes entry by binding vinculin, but an *ipaA* mutant still invades at low frequency (5). Actin rearrangements promoted by the small Rho GTPases Cdc42 and Rac1 contribute to entry, yet expression of dominant negative forms of either decreases entry by only ~70% (6). Activation of the Rac1 guanine exchange factor (GEF) DOCK180/ELMO by *Shigella* IpgB1 contributes to entry, yet an *ipgB1* mutant invades at 35% of the efficiency of the wild type (WT) (7, 8).

GTPases are molecular switches that transduce signals to regulate functions as diverse as gene expression, vesicular trafficking, and cytoskeletal rearrangement (9) and are manipulated by several bacterial pathogens (10). GTPases of the ADP-ribosylation factor (ARF) family act at the plasma membrane and at endosomes to regulate membrane trafficking, phosphoinositide and lipid metabolism, and actin remodeling (11, 12). Distinct from other ARF GTPases in amino acid sequence and intracellular localization, GTP-bound ARF6 is localized to the plasma membrane and on endosomes, where it activates phosphatidylinositol 4-phosphate 5-kinase (PIP5K), generating phosphatidylinositol 4,5-bisphosphate [$PI(4,5)P_2$] (13–15). In motile cells, ARF6 also promotes actin remodeling via activation of Rac1, dependent on

the GEFs ARF nucleotide binding site opener (ARNO) and DOCK180/ELMO complex (16–19).

The localization of ARF6 at the plasma membrane and its role in membrane trafficking and actin remodeling during endocytosis place it in an ideal position to participate in pathogen uptake and endosome remodeling (18–22). The mechanism of ARF6 recruitment and activation has not been described for any pathogen.

We report a role for ARF6 in a previously undescribed positive feedback loop that amplifies ARF6 activation to promote *Shigella flexneri* entry. We find that ARF6 is activated during *S. flexneri* entry and is required for efficient entry. We show that the ARF GEF ARNO lies upstream of ARF6 in this pathway and that the activity of the T3SS effector IpgD, an inositol 4-phosphatase (23–25), is required for recruitment of both ARF6 and ARNO to bacterial entry sites. These findings provide new insights into the mechanism of GTPase recruitment and activation during bacterial entry.

RESULTS

ARF6 is required for efficient entry of *S. flexneri*. To test whether ARF6 contributes to *S. flexneri* infection, we quantified the efficiency of infection in HeLa cells transfected with wild-type (WT) hemagglutinin (HA)-tagged ARF6 or ARF6 N122I, a dominant negative mutant unable to bind guanine nucleotides (21). At 2 h of infection, the number of intracellular bacteria in cells expressing ARF6 N122I was 30% less than in cells expressing WT ARF6 (7.2 ± 0.1 versus 5.1 ± 0.2 intracellular bacteria per transfected cell, $P = 0.001$) (Fig. 1A), demonstrating that entry and/or early intracellular replication of *S. flexneri* is less efficient in the presence of dominant negative ARF6. To test whether ARF6 *per se* is required for efficient infection, we examined infection in mouse embryonic fibroblasts (MEFs) that harbor a stable lentiviral short hairpin RNA (shRNA) construct targeting *Arf6* mRNA ($ARF6^{K/D}$) (26), such that levels of ARF6 are reduced by >90% compared to control cells ($ARF6^{+}$) that harbor a nontargeting lentiviral insertion (see Fig. S1A in the supplemental material). Viable intracellular *S. flexneri* levels in $ARF6^{K/D}$ MEFs were 2-fold decreased compared to $ARF6^{+}$ MEFs at 1 and 2 h of infection (at 1 h, 1,327 ± 311 CFU versus 651 ± 147 CFU, $P = 0.03$; at 2 h, 11,027 ± 1,430 CFU versus 5,188 ± 193 CFU, $P = 0.03$) (Fig. 1B). Thus, in both HeLa cells and MEFs, in the absence of ARF6, entry and/or early intracellular replication of *S. flexneri* is less efficient.

S. flexneri entry into cells occurs as early as 15 min after bacterial contact with the host cell (27, 28). To test whether ARF6 is required for *S. flexneri* entry *per se*, we quantified the percentage of intracellular bacteria 40 min after initial contact with cells, before significant replication of intracellular bacteria would have occurred, differentiating extracellular bacteria from those that were intracellular by differential labeling. Extracellular bacteria were identified by labeling with *S. flexneri* lipopolysaccharide (LPS) prior to cell permeabilization, whereas all bacteria were identified by staining DNA with 4′,6-diamidino-2-phenylindole (DAPI). At 40 min of infection, the number of cells infected by *S. flexneri* was decreased by 75% in $ARF6^{K/D}$ MEFs compared to $ARF6^{+}$ MEFs (32% ± 8.6% versus 8% ± 0.6% of cells were infected, $P = 0.03$) (Fig. 1C and D, left graph). When transiently transfected with an HA-tagged WT ARF6 construct, $ARF6^{K/D}$ MEFs exhibited partial restoration of ARF6 protein levels (see Fig. S1A in the supplemental material). The relatively minor rescue in levels was likely due to the combination of only a portion of the cells having been transfected and the susceptibility of the ARF6-HA RNA to the shRNA expressed in the $ARF6^{K/D}$ cells. Nevertheless, transient transfection of this construct resulted in rescue of bacterial entry to that in $ARF6^{+}$ MEFs (Fig. 1D, right graph), suggesting that relatively low levels of ARF6 are sufficient to promote entry and demonstrating that efficient *S. flexneri* entry is dependent on ARF6.

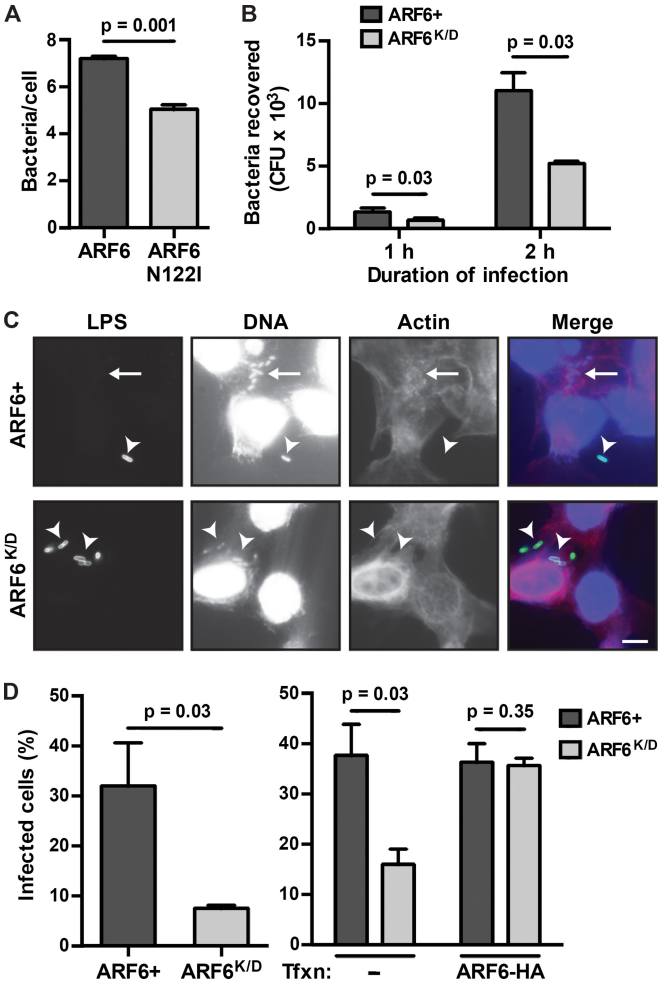

FIG 1 ARF6 is required for efficient entry of *S. flexneri*. (A) Efficiency of infection of HeLa cells transfected with ARF6-HA or dominant negative ARF6 N122I-HA. Number of intracellular bacteria per cell at 2 h of infection, by differential staining. (B) *S. flexneri* recovered after infection (1 or 2 h) of $ARF6^{K/D}$ or $ARF6^{+}$ MEFs, by gentamicin protection assay. (C and D, left graph) Early infection (40 min) of $ARF6^{K/D}$ or $ARF6^{+}$ MEFs, with differential staining of extracellular versus intracellular bacteria. Extracellular bacteria stained with antibody to LPS (green) and all bacteria identified by DAPI (DNA, blue). Phalloidin staining of polymerized actin (red). Images are representative. Arrows, intracellular bacteria. Arrowheads, extracellular bacteria. Bar, 10 μm. (D, right graph) Rescue of *S. flexneri* entry by transient transfection of $ARF6^{K/D}$ MEFs with ARF6-HA. Efficiency of entry into ARF6-HA-transfected cells was for the subset of cells that expressed ARF6-HA. Mean ± standard error of the mean of at least 3 independent experiments.

Virulent *S. flexneri* activates ARF6 during early infection. Like most small GTPases, in resting cells, ARF6 is predominantly in the GDP-bound inactive form. The requirement for ARF6 for efficient *S. flexneri* entry suggested that ARF6 might be activated during this process. To quantify ARF6 activation, GTP-bound

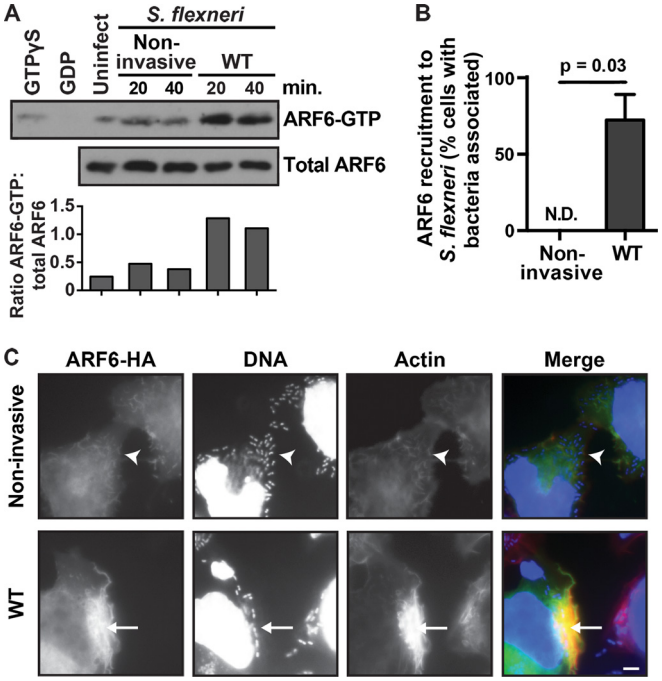

FIG 2 Virulent *S. flexneri* activates ARF6 early during infection. (A) ARF6 activation determined by pulldown of GTP-bound ARF6 from HeLa cells 20 or 40 min after initial contact of WT or noninvasive *S. flexneri* (top panel) with cells, versus total ARF6 in each lysate (bottom panel). GTPγS or GDP added to lysates of uninfected cells and uninfected cells alone (uninfect) are positive and negative controls. Ratio of ARF6-GTP to total ARF6 for blots shown, by densitometry. Blots are representative. (B and C) ARF6-HA recruitment to AFA-I-expressing WT or noninvasive *S. flexneri* in HeLa cells infected (40 min), fixed, and stained with antibody to HA (green), DAPI (blue), and phalloidin (red). ND, not detectable. Mean ± standard error of the mean for 3 independent experiments. Images are representative. Arrows, ARF6 recruitment to entering bacteria. Arrowheads, bacteria without ARF6 recruitment. Bar, 10 μm.

ARF6 was precipitated from lysates of infected cells using beads conjugated to the ARF binding domain of Golgi complex-associated, gamma adaptin ear-containing ARF binding protein 3 (GGA3), which specifically binds GTP-bound ARF6 (29). WT *S. flexneri* induced activation of ARF6 as early as 20 min after contact with HeLa cells, whereas a strain that is noninvasive by virtue of lacking the virulence plasmid did not activate ARF6 at either time assessed (Fig. 2A), indicating that *S. flexneri* activates ARF6 soon after cell contact and in a manner that depends on virulence plasmid-encoded factors.

Exchange of bound GDP for GTP activates ARF6 and recruits it from a cytosolic pool to the plasma membrane (30–32), suggesting that ARF6 activation during *S. flexneri* entry might be associated with its recruitment to entry sites. WT *S. flexneri* recruited HA-tagged ARF6 to bacteria at the plasma membrane early in infection (40 min), but the noninvasive strain did not (85% versus <1% of cells displayed ARF6 recruitment to bacteria, $P = 0.03$) (Fig. 2B and C). In this experiment, to ensure that bacterial contact with the plasma membrane occurred independently of type III secretion, we used strains that adhered tightly as a result of heterologous production of the uropathogenic *Escherichia coli* afimbrial adhesin (AFA-I); as a result, every cell displayed adherent bacteria. *S. flexneri* similarly recruited ARF6-HA in MEFs (18% versus <1% of cells with bacteria associated showed ARF6 recruitment to bacteria, $P = 0.001$) (see Fig. S2 in the supplemental material); here, only a subset of cells displayed adherent bacteria, as AFA-I was not used because its receptor is absent in murine cells. These results show that ARF6 activation by *S. flexneri* is associated with its recruitment to bacterial entry sites and is dependent not simply on contact with the plasma membrane but rather on virulence plasmid-encoded factors.

The phosphoinositide phosphatase activity of *Shigella* T3SS effector IpgD is required for efficient ARF6 activation at entry sites. We tested whether any of several effector proteins secreted into cells by the *S. flexneri* virulence plasmid-encoded type III secretion system (T3SS) were required for activation of ARF6. We postulated that the involved effector was likely to either possess GTPase exchange factor (GEF) activity or recruit an ARF GEF to entry sites. We therefore focused on the effectors IpgB1, IpgB2, IpgD, and IpaJ. IpgB1 and IpgB2 possess GEF activity; IpgB1 principally activates the host GTPases Rac1 and Cdc42, and IpgB2 principally activates RhoA, yet the two effectors are homologous with some overlap in function (8, 33, 34). IpgD is an inositol 4-phosphatase with no known homology to effectors with GEF activity but, like IpgB1, is translocated early upon bacterial contact with host cells and participates in actin remodeling at entry sites (7, 23, 24). Moreover, the substrate of IpgD, $PI(4,5)P_2$, is concentrated at the plasma membrane (35). IpaJ demyristoylates ARF1 (36), an ARF GTPase that is 66% identical to ARF6 (11).

To test whether any of these effectors is required for *S. flexneri*-induced ARF6 activation, we examined the ability of strains lacking each individually to activate ARF6 during entry. Whereas the other mutant strains examined activated ARF6 at levels comparable to the WT strain, the Δ*ipgD* mutant was defective in ARF6 activation (Fig. 3A). We then tested whether IpgD was required for ARF6 recruitment to bacterial entry sites by specifically assessing the efficiency of ARF6 recruitment to sites where bacteria were adherent to cells and/or within a membrane ruffle, reasoning that these constituted the bulk of the bacterial population potentially undergoing cellular entry. Compared to WT, the Δ*ipgD* mutant was defective in ARF6 recruitment (57% versus 38% of cells with bacteria associated showed ARF6 recruitment, $P = 0.04$) (Fig. 3B, left graph). The ARF6 recruitment defect was rescued by *ipgD* expressed in *trans*, but not by expression of *ipgD* C438S, a catalytically dead mutant with no phosphatase activity (24) (54% and 7% of cells with bacteria associated showed ARF6 recruitment, respectively, $P = 0.003$) (Fig. 3B, right graph, and C). These results demonstrate that IpgD phosphatase activity is critical for ARF6 activation and for ARF6 recruitment to bacterial entry sites.

The Δ*ipgD* mutant was defective in entry (17% of cells infected by Δ*ipgD* mutant versus 31% of cells infected by WT, $P = 0.002$) (Fig. 3D, left graph), and the entry defect was rescued by WT IpgD but not by IpgD C438S (68% versus 21% of cells infected, respectively; $P = 0.0006$) (Fig. 3D, right graph). Thus, IpgD phosphatase activity is required both for activation of ARF6 and for efficient entry. The Δ*ipgD* mutant was defective in the formation of plasma membrane ruffles at entry sites (25% versus 12% of cells displayed bacteria in a ruffle; $P = 0.001$) (Fig. 3E, left graph). IpgD but not IpgD C438S rescued the ruffling defect (46% and 4% of cells displayed bacteria in a ruffle, respectively; $P = 0.0016$) (Fig. 3E, right graph). Both the Δ*ipgD* mutant complemented with WT IpgD

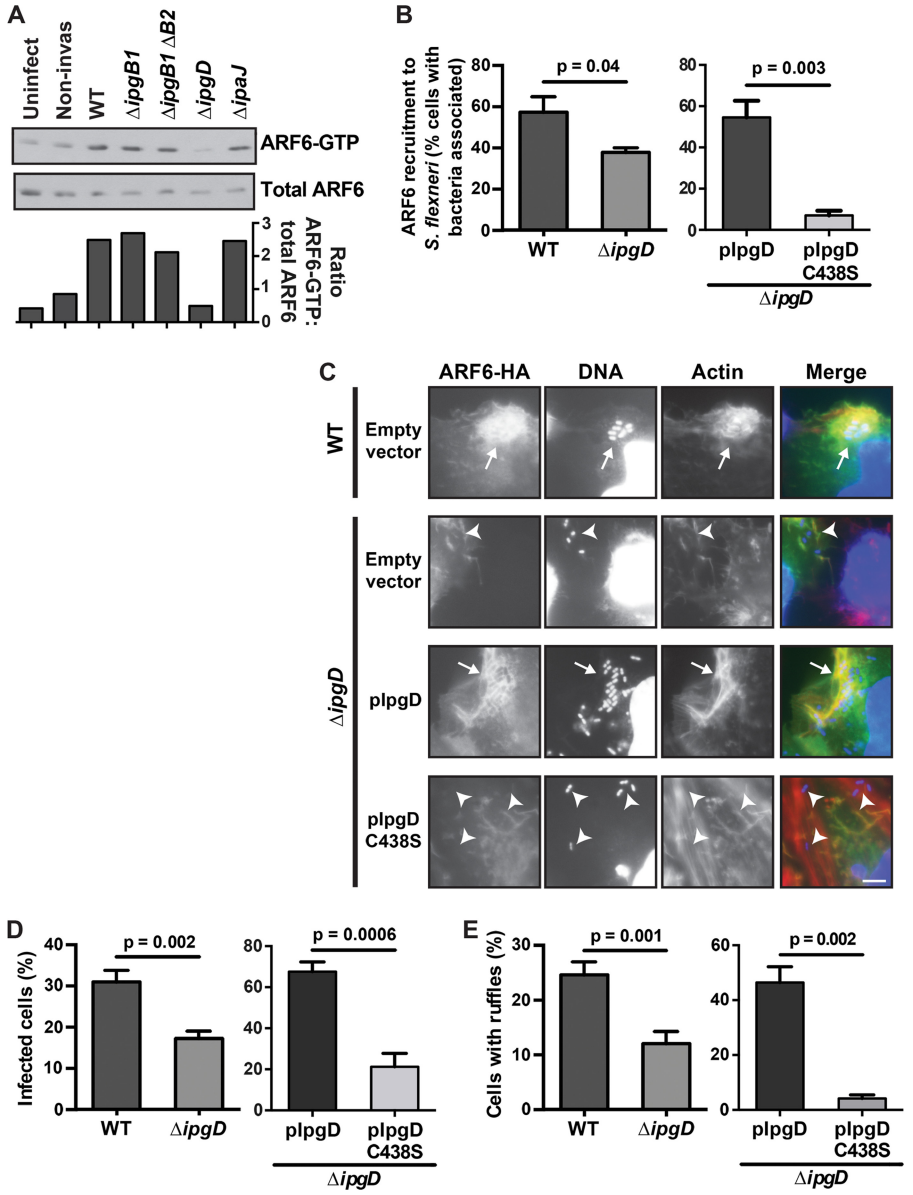

FIG 3 The phosphoinositide phosphatase activity of *Shigella* T3SS effector IpgD is required for efficient ARF6 activation at entry sites. (A) ARF6 activation determined by pulldown of GTP-bound ARF6 from HeLa cells infected with indicated *S. flexneri* strains for 40 min after initial bacterial contact with cells (top panel) versus total ARF6 in each lysate (bottom panel). Ratio of ARF6-GTP to total ARF6 for blots shown, by densitometry. Uninfect, uninfected; Non-invas, noninvasive strain; Δ*ipgB1* Δ*B2*, Δ*ipgB1* Δ*ipgB2* mutant. Blots are representative. (B to E) Infection of ARF6-HA-transfected HeLa cells (40 min) with WT, Δ*ipgD*, Δ*ipgD* pIpgD, or Δ*ipgD* pIpgD C438S *S. flexneri*, fixed and labeled with antibody to HA (green), DAPI (blue), and phalloidin (red). (B) Percentage of cells with bacteria associated that show ARF6 recruitment to bacteria. (C) Representative images. Arrows, bacteria with ARF6 recruitment. Arrowheads, bacteria without ARF6 recruitment. Bar, 10 μM. (D and E) Percentage of cells infected or with ruffles. Mean ± standard error of the mean of at least 3 independent experiments.

and that complemented with IpgD C438S produced IpgD at higher levels than the WT strain (see Fig. S3 in the supplemental material), likely due to plasmid copy number. In the presence of overexpression of WT IpgD, entry and ruffle formation were more efficient, whereas overexpression of IpgD C438S was associated with an apparent dominant negative effect on entry and ruffle formation, further confirming a role for IpgD and IpgD phosphatase activity in *S. flexneri* entry.

Efficient ARF6 recruitment to entering *S. flexneri* requires cytohesin GEFs. GEFs activate small GTPases such as ARF6 by stimulating GDP dissociation, which allows GTP binding. In the absence of homology that might suggest intrinsic GEF activity, a mechanism by which IpgD might promote ARF6 activation is by recruiting and/or activating an ARF6 GEF at *S. flexneri* entry sites. Known GEFs of ARF6 include BRAG1, GEP100/BRAG2, EFA6, and the cytohesin GEFs, cytohesin-1, ARNO (cytohesin-2), and GRP1 (cytohesin-3) (37–41). We tested whether cytohesin GEFs are required for *S. flexneri* entry and for ARF6 recruitment to entering bacteria by treating cells with SecinH3, a small-molecule cytohesin family-specific inhibitor (42) that inhibits all cytohesin

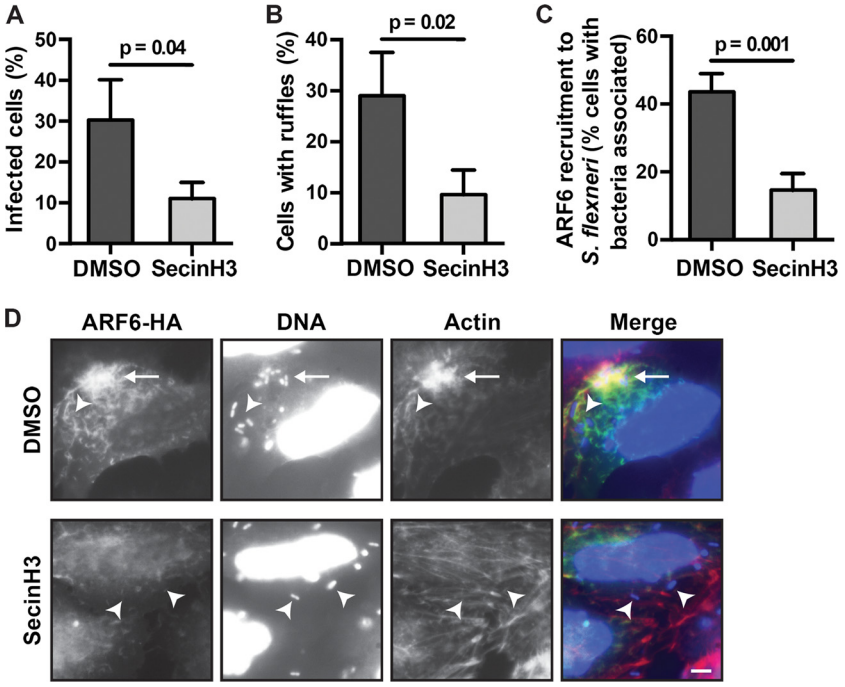

FIG 4 Efficient ARF6 recruitment to entering *S. flexneri* requires cytohesin GEFs. Recruitment of ARF6-HA to HeLa cells infected with *S. flexneri* for 40 min in the presence of SecinH3 or dimethyl sulfoxide (DMSO). (A) Percentage of cells infected. (B) Percentage of cells with ruffles. (C) Percentage of cells with bacteria associated showing ARF6 recruitment to bacteria. Mean ± standard error of the mean of at least 3 independent experiments. (D) Representative images with labeling with antibody to HA (green), DAPI (blue), and phalloidin (red). Arrows, bacteria with ARF6 recruitment. Arrowheads, bacteria without ARF6 recruitment. Bar, 10 μm.

family GEFs. Cytohesin-1 is highly expressed in natural killer T lymphocytes (43), whereas ARNO and GRP1 have roles in epithelial cells (17, 44). SecinH3 inhibited *S. flexneri* entry (30% versus 11% of cells were infected; $P = 0.04$) (Fig. 4A) and ruffle formation (29% versus 10% of cells displayed bacteria in a ruffle; $P = 0.02$) (Fig. 4B), indicating that one or more cytohesin GEFs contribute to entry. SecinH3 inhibited *S. flexneri* entry not only in the presence of ARF6 (29% versus 14% of ARF6$^+$ MEFs were infected, $P = 0.03$) but also in its absence (16% versus 8% of ARF6$^{K/D}$ MEFs were infected, $P = 0.02$) (data not shown); since ARNO can activate ARF1 downstream of ARF6 (18, 19), we speculate that this SecinH3-induced decrease in infection of ARF6$^{K/D}$ MEFs may be due to inhibition of ARNO-dependent activation of ARF1.

To determine whether cytohesin GEFs were functioning upstream of ARF6 in *S. flexneri* entry, we tested whether ARF6 recruitment depended on cytohesin activity. In the presence of SecinH3, ARF6 recruitment to potential entry sites was decreased (44% versus 15% of cells with bacteria associated showed ARF6 recruitment to bacteria; $P = 0.001$) (Fig. 4C and D), demonstrating that SecinH3 blocked efficient ARF6 activation by *S. flexneri*. Thus, cytohesin GEF activity is critical to efficient ARF6 activation by entering *S. flexneri* and to efficient bacterial entry, consistent with the inhibitory effect of SecinH3 on entry being due at least in part to inhibition of ARF6 activation.

Interaction of IpgB1 with ELMO, a component of the Rac1 GEF DOCK180/ELMO complex, promotes bacterial uptake (7). ARNO is required for activation of DOCK180/ELMO (17). Whether ARNO activation of DOCK180/ELMO depends on ARF6 is unclear. These observations, in conjunction with the observed effects of SecinH3 on *S. flexneri* activation of ARF6 and entry, led us to postulate that ARNO might participate in activation of ARF6. Myc-tagged ARNO was recruited to *S. flexneri* entry sites. Experimental optimization suggested that membrane ruffling and ARF6 recruitment both peak within 30 to 40 min after initial bacterial contact with HeLa cells, whereas ARNO recruitment peaks approximately 10 min earlier (data not shown). ARNO recruitment in HeLa cells depended on the presence of the virulence plasmid, even for bacteria that expressed the AFA-I adhesin (55% of cells for WT versus <1% of cells for noninvasive strain displayed ARNO recruitment to bacteria; $P = 0.001$) (Fig. 5A and B).

Since ARNO recruitment apparently preceded ARF6 recruitment, we tested whether ARNO recruitment might be independent of ARF6 by examining its recruitment in ARF6$^+$ and ARF6$^{K/D}$ MEFs. ARNO exists as two splice variants—ARNO 2G and ARNO 3G—that differ by the addition of a single glycine residue in the phosphoinositide-binding pocket of the ARNO pleckstrin homology (PH) domain (45). Because the two variants display distinct binding preferences for phosphoinositide species at the membrane (45, 46), we separately examined the recruitment of each. Each ARNO variant was independent of ARF6 for recruitment to entering bacteria (42% each of cells with bacteria associated showed ARNO 2G recruitment to bacteria in ARF6$^+$ and ARF6$^{K/D}$ MEFs, respectively; $P = 1.0$; for ARNO 3G, 42% versus 35%, respectively; $P = 0.3$) (Fig. 5C and D), indicating that ARNO is recruited upstream of ARF6, which positions it to potentially contribute to activation of ARF6 at sites of *S. flexneri* entry. These findings are notably different from what has been observed during *Salmonella* infection, where ARNO recruitment to entry sites is

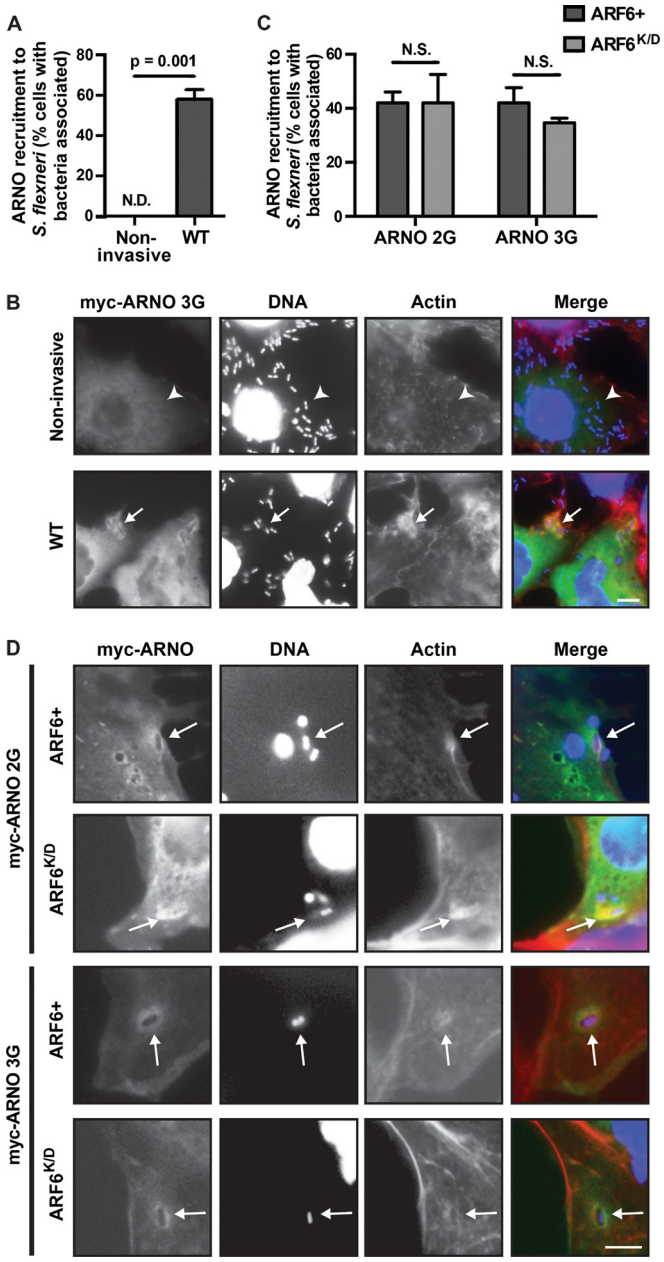

FIG 5 ARNO is recruited to entering *S. flexneri* independent of ARF6. (A and B) Recruitment of Myc-ARNO 3G to AFA-I-expressing WT or noninvasive *S. flexneri* in HeLa cells, infected for 30 min. Representative images labeled with antibody to Myc (green), DAPI (blue), and phalloidin (red). (C and D) Recruitment of Myc-ARNO 2G or Myc-ARNO 3G to *S. flexneri* entering ARF6$^{K/D}$ or ARF6^{+} MEFs, infected for 25 min. Labeling as in panel B. Arrows, entering bacteria with ARNO recruitment. Arrowheads, bacteria without ARNO recruitment. ND, not detectable. NS, not significant. Mean ± standard error of the mean of at least 3 independent experiments. Bars, 10 μm.

defective in the absence of ARF6 (19); the reasons for these organism-based differences are at present unclear.

IpgD and IpgD phosphatase activity are required for ARNO recruitment to entry sites and *S. flexneri* entry. IpgD-induced PI(5)P accumulation activates PI 3-kinase (PI3K), leading to generation of phosphatidylinositol 3,4,5-trisphosphate [PI(3,4,5)P_3] (47). The PH domains of ARF GEFs bind phosphoinositides with various affinities; these interactions recruit GEFs to the plasma membrane (37, 48–50). We considered that recruitment of ARNO to *S. flexneri* entry sites might be enhanced by IpgD-mediated generation of phosphoinositide species that bind ARNO with high affinity. IpgD was required for recruitment of ARNO to entry sites (cells with bacteria associated showing ARNO recruitment to bacteria, 59% for WT versus 20% for Δ*ipgD* mutant, $P = 0.001$) (Fig. 6A, left graph). IpgD but not IpgD C438S rescued ARNO recruitment by the Δ*ipgD* mutant (44% and 5% of cells with bacteria associated showed ARNO recruitment to bacteria, respectively) (Fig. 6A, right graph, and B). In the absence of IpgD, ARNO recruitment was more dramatically reduced than ARF6 recruitment (Fig. 6A, left graph, versus 3B), likely due to a contribution of other SecinH3-sensitive ARF6 GEFs to ARF6 recruitment, since knockdown of ARNO alone did not lead to significant decreases in ARF6 recruitment (see Fig. S4 in the supplemental material). As above (Fig. 3D and E), the phosphatase activity of IpgD was required for both efficient entry and membrane ruffling at entry sites (see Fig. S5 in the supplemental material). Moreover, PI(3,4,5)P_3 was generated at *S. flexneri* entry sites, as assessed by recruitment of a green fluorescent protein (GFP)-tagged pleckstrin homology domain from Bruton's tyrosine kinase (BTK-PH-GFP), which specifically binds PI(3,4,5)P_3 (51), and efficient generation of PI(3,4,5)P_3 was dependent on IpgD (Δ*ipgD* mutant, 18%, versus WT, 37%, for cells displaying BTK-PH-GFP recruitment to entry sites, $P = 0.04$) (Fig. 6C and D). Thus, the phosphatase activity of IpgD is critical for both generation of PI(3,4,5)P_3 at entry sites and ARNO recruitment, and IpgD and SecinH3-sensitive GEFs are each required for ARF6-mediated *S. flexneri* entry.

Recruitment to entry sites of ARNO 2G but not ARNO 3G is defective upon inhibition of PI3K. These data raised the possibility that IpgD-dependent changes in phosphoinositide composition, specifically PI3K-dependent generation of PI(3,4,5)P_3, contribute to recruitment of ARNO to bacterial entry sites. We tested whether inhibition of PI3K by addition of the chemical inhibitor LY294002 to cells during bacterial entry altered recruitment of ARNO. Recruitment of ARNO 2G, which preferentially binds PI(3,4,5)P_3, was defective in the presence of LY294002 (29% versus 50% of cells with bacteria attached displaying ARNO recruitment, $P = 0.04$) (Fig. 6E, left graph, and F), whereas recruitment of ARNO 3G, which binds PI(4,5)P_2 with high affinity (45, 46), was unaffected (30% versus 36%, $P = 0.4$) (Fig. 6E, right graph). Treatment of cells with LY294002 was associated with defective phosphorylation of Akt (see Fig. S6 in the supplemental material), confirming that the conditions used inhibited PI 3-kinase activity. Thus, IpgD-dependent generation of PI(3,4,5)P_3 during entry of *S. flexneri* enhances recruitment of the 2G variant of the ARF6 GEF ARNO.

DISCUSSION

Our findings, combined with published data, support the presence of a positive feedback loop that promotes ARF6 activation during *S. flexneri* entry into cells. We demonstrate that activation of ARF6 is required for efficient entry of *S. flexneri* into both epithelial cells and MEFs, that ARF6 activation depends on phosphatase activity of the T3SS effector IpgD, and that the cytohesin ARF6 GEF ARNO is recruited upstream of ARF6 where it contributes to ARF6 activation (Fig. 7). ARF6 activation is known to drive Rac1-dependent actin remodeling, which promotes membrane

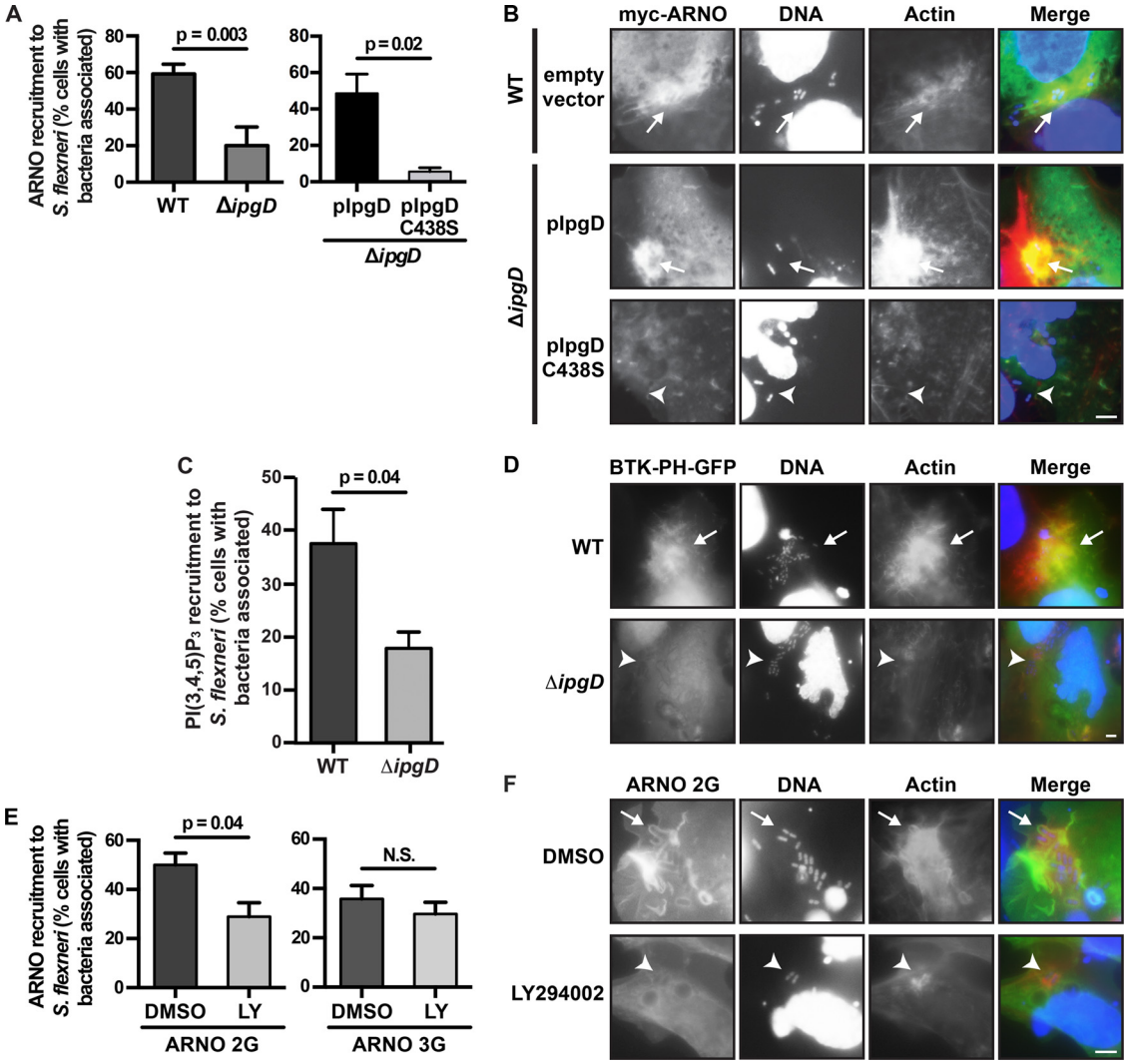

FIG 6 IpgD phosphatase activity is required for ARNO recruitment to entry sites, and PI 3-kinase contributes to ARNO 2G but not ARNO 3G recruitment. (A and B) WT, Δ*ipgD*, Δ*ipgD* pIpgD, and Δ*ipgD* pIpgD C438S *S. flexneri* infection for 30 min of HeLa cells transfected with Myc-ARNO 3G. (A) Percentage of cells with ARNO recruitment to entering bacteria. (B) Representative images, labeled with antibody to Myc (green), DAPI (blue), and phalloidin (red). (C and D) Recruitment of PI(3,4,5)P_3 to bacterial entry sites upon WT or Δ*ipgD* infection for 40 min of HeLa cells transfected with BTK-PH-GFP, which specifically binds PI(3,4,5)P_3. (C) Percentage of cells with BTK-PH-GFP recruitment to entering bacteria. (D) Representative images, labeled with DAPI (blue), and phalloidin (red), and with GFP signal. (E and F) Inhibition of recruitment of ARNO 2G, but not ARNO 3G, upon treatment with LY294002 upon WT infection of ARF6$^{K/D}$ MEFs for 25 min. (E) Percentage of cells with ARNO recruitment to entering bacteria. (F) Representative images, labeled as in panel B. Arrows, bacteria with ARNO recruitment. Arrowheads, bacteria without ARNO recruitment. Bars, 10 μm. NS, not significant. Mean ± standard error of the mean of at least 3 independent experiments. DMSO, dimethyl sulfoxide; LY, LY294002.

ruffle formation and bacterial entry (16, 17). Thus, the amplification of signals immediately beneath sites of bacterial contact with the plasma membrane that result from this positive feedback loop would be expected to promote rapid local changes that facilitate bacterial entry.

In a positive feedback loop, amplification allows the output signal to reach a critical threshold at which the system switches from one state to another, traditionally basal to active (52). Positive feedback loops have been reported for Rab (53, 54) and ARF (55, 56) GTPase signaling. ARNO recruitment to the plasma membrane is by two distinct mechanisms: binding to phosphoinositides and phosphatidylserine and binding to ARF6 (57, 58). In an ARF6 feedback loop, GTP-bound ARF6 stimulates ARNO, and ARNO activates ARF1 and is then stimulated by GTP-bound ARF1 (55). Cohen et al. found that GTP-bound ARF6 binds the ARNO PH domain, leading to ARNO recruitment to the plasma membrane and activation of ARF1 (57). Cascades of GEFs and GTPases can thus constitute positive feedback loops that feed back onto themselves.

The positive feedback loop that our data support is distinct from described GEF cascades in that IpgD phosphatase activity generates signals that contribute to GEF recruitment. These signals include the generation of membrane-anchored phosphoinositide species that bind ARNO. Since PI(4,5)P_2, the substrate for IpgD phosphatase activity, is generated by ARF6-mediated activation of PIP5K, by our model, IpgD activity is fueled by its ability to generate phosphoinositides that enhance ARNO recruitment. Moreover, because inactive ARF6 does not bind the ARNO PH

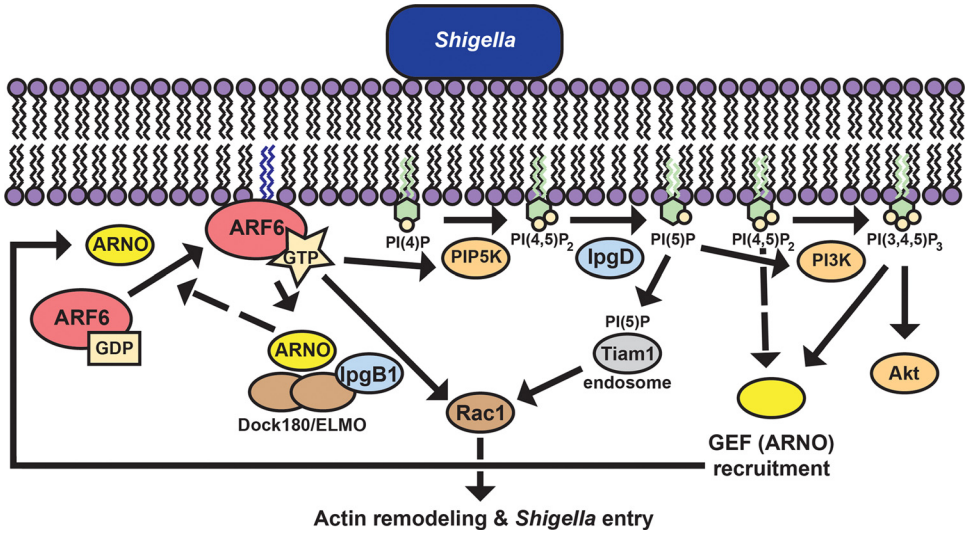

FIG 7 Model of IpgD-dependent positive feedback loop that amplifies ARF6 activation during entry of *S. flexneri*. Extracellular *S. flexneri* recruits ARNO to the plasma membrane in part via IpgD-induced local accumulation of $PI(3,4,5)P_3$. ARNO-dependent activation of ARF6 induces PIP5K-mediated changes in phosphoinositide composition at the membrane that promote additional ARNO recruitment, mediating further activation of ARF6. Solid arrows, relationships supported by data presented here or previously published. Dashed arrows, postulated relationships.

domain (57), IpgD-generated phosphoinositides may function as the seed for ARNO recruitment and subsequent ARF6 recruitment and activation. This model, supported by the data presented here, predicts that IpgD activity expands the existing GEF-ARF cascade in a manner that further amplifies ARF6 activation.

Our findings establish a substantial expansion of the model of ARF GTPase participation in entry, previously described for *Salmonella enterica* serovar Typhimurium by Humphreys et al. (18, 19). Data from the prior studies support a model in which ARF6 recruits ARNO, ARNO in turn recruits ARF1, and ARF1 promotes actin polymerization via the WAVE regulatory complex (18, 19). In our work here, in addition to showing that entry by *S. flexneri* parallels that of *S. Typhimurium* with respect to participation of ARF GTPases, we characterize for the first time a mechanism of activation of ARF6 in this process and demonstrate the presence of the previously undescribed positive feedback loop that likely amplifies ARF6 activation. Moreover, our results identify an important difference from the entry of *S. Typhimurium*, wherein ARNO recruitment is dependent on ARF6 (19), in that during entry of *S. flexneri*, ARNO recruitment is independent of and occurs upstream of ARF6. Although the reasons are currently unclear, these findings may highlight the existence of important functional divergence between *Shigella* and *Salmonella*.

An important insight that emerges from our data together with published data (18, 19) is that during bacterial entry, ARNO participates in the activation of both ARF6 and ARF1, which lies downstream of ARF6. Thus, ARF GEFs such as ARNO (but perhaps not restricted to ARNO) may participate promiscuously at multiple steps during bacterial infection. ARNO recruitment was absolutely dependent on IpgD. The effector IpgB1 recruits the Rac1 GEF DOCK180/ELMO to entry sites (7). DOCK180/ELMO is activated by ARF6 via ARF1 and dependent on ARNO GEF activity (17, 19).

$PI(4,5)P_2$ is relatively abundant in both resting and stimulated cells, whereas $PI(3,4,5)P_3$ is detectable only following stimulation (59). IpgD phosphatase activity leads to the recruitment of $PI(3,4,5)P_3$ (Fig. 6C and D). $PI(4,5)P_2$ and $PI(3,4,5)P_3$ bind PH domains of ARF GEFs. The high-affinity interaction of membrane-anchored $PI(3,4,5)P_3$ with the ARNO 2G variant is sufficient to recruit it to the plasma membrane, whereas the low-affinity interaction of $PI(3,4,5)P_3$ with the ARNO 3G variant is not sufficient (45, 60, 61). In brain tissue, the 3G variant of ARNO is most abundant (46); the relative abundance of the two variants in other tissues is unknown.

Recruitment of ARNO to *S. flexneri* entry sites is dependent on IpgD phosphatase activity (Fig. 6A to C) and independent of ARF6 (Fig. 5). The reduction in recruitment of the 2G variant of ARNO upon chemical inhibition of PI 3-kinase (Fig. 6E and F) is consistent with a model in which transient $PI(3,4,5)P_3$ accumulation, induced by IpgD-dependent activation of PI 3-kinase, leads to efficient recruitment of ARNO 2G via its high-affinity interaction with $PI(3,4,5)P_3$. However, recruitment of ARNO 3G is independent of $PI(3,4,5)P_3$ accumulation (Fig. 6D) and thus must be mediated by other factors that accumulate at entry sites in response to IpgD phosphatase activity.

Our data demonstrate for the first time that IpgD is required for efficient *S. flexneri* entry. Of note, although statistically significant, the defect in entry of the *ipgD* mutant is relatively minor (Fig. 3D). That the relatively small defect is meaningful is supported by the enhanced entry observed upon overexpression of IpgD (Fig. 3D). The presence of only a minor defect is also consistent with several lines of evidence that point to *Shigella* entry resulting from multiple partially redundant mechanisms mediated by various T3SS effectors (5, 7, 8). The relatively small decrease observed, along with differences in strain backgrounds, likely explains why the role of IpgD in entry has been unappreciated in other experimental systems (62, 63).

IpgD phosphatase activity and the phosphoinositides that it generates have previously been implicated in *S. flexneri* activation of Akt (47), regulation of vesicular trafficking (64), recruitment of Rab-11-containing vesicles to bacterial uptake vacuoles (63), inhibition of chemokine-induced migration of T

TABLE 1 Bacterial strains and plasmids used in this study

Strain or plasmid	Genotype or description	Reference or source
Bacterial strains		
Wild type	Serotype 2a *S. flexneri* strain 2457t	68
Noninvasive	BS103 (2457T cured of its virulence plasmid)	71
Wild type with adhesin	2457T pIL22, Amp^r	Lab stock
Noninvasive with adhesin	BS103 pIL22, Amp^r	Lab stock
Δ*ipgD* mutant	2457T *ipgD*::FRT-Km^r-FRT[a]	Gift of C. Lesser
Δ*ipgD* pIpgD mutant	2457T *ipgD*::FRT-Km^r-FRT pACYC184 *ipgD-ipgE*	This study
Δ*ipgD* pIpgD C438S mutant	2457T *ipgD*::FRT-Km^r-FRT pACYC184 *ipgD* C438S-*ipgE*	This study
Δ*ipgB1* mutant	2457T *ipgB1*::FRT	Lab stock
Δ*ipgB1* Δ*ipgB2* mutant	2457T *ipgB1*::FRT *ipgB2*::FRT	Lab stock
Δ*ipaJ* mutant	2457T *ipaJ*::FRT	Lab stock
Plasmids		
pACYC184	Cm^r	Lab stock
pIpgD	pACYC184 *ipgD-ipgE*, Cm^r	This study
pIpgD C438S	pACYC184 *ipgD* C438S-*ipgE*, Cm^r	This study
pIL22	pBR322 encoding *Escherichia coli* afimbrial adhesin AFA-I, Amp^r	72
ARF6-HA	pcDNA HA-tagged ARF6, Amp^r	21
ARF6 N122I-HA	pcDNA HA-tagged ARF6 defective for nucleotide binding, Amp^r	21
BTK-PH-GFP	pEGFP-N1-BTK-PH-GFP, Km^r	51
Myc-ARNO 3G	pcDNA3 Myc-tagged ARNO, 3G variant, Amp^r	29
Myc-ARNO 2G	pcDNA3 Myc-tagged ARNO, 2G variant, Amp^r	Gift of L. Santy

[a] FRT, FLP recombination target.

cells (65), inhibition of ATP release through connexin hemichannels (66), and activation of the GEF Tiam1 in Rac1-mediated actin rearrangements (67). Our data now add to the list a role in entry via activation of ARF6. The multiple effects of IpgD during *S. flexneri* infection highlight the central role that phosphoinositides play in intracellular signaling and the extent to which *S. flexneri* has evolved mechanisms to manipulate these signaling pathways.

MATERIALS AND METHODS

Bacterial strains, plasmids, and growth conditions. Strains and plasmids are listed in Table 1. All *S. flexneri* strains are isogenic to serotype 2a wild-type strain 2457T (68). *S. flexneri* bacteria were grown at 37°C in tryptic soy broth from individual Congo red-positive colonies. Antibiotics were ampicillin (Amp), 100 μg/ml; chloramphenicol (Cm), 25 μg/ml; and kanamycin (Km), 50 μg/ml. To generate pIpgD and pIpgD C438S, the coding sequences of *ipgD*, its promoter, and its chaperone *ipgE* were cloned into pACYC184 with site-directed mutagenesis of pIpgD (QuikChange mutagenesis kit; Stratagene).

Cell culture. HeLa cells were cultured in high-glucose Dulbecco's modified Eagle's medium (DMEM; Gibco), and ARF6$^{K/D}$ and ARF6$^+$ mouse embryonic fibroblasts (MEFs) (gift of Wim Annaert [26]) were cultured in DMEM–nutrient mixture F-12, each with 10% fetal bovine serum. Monolayers were transfected 24 h prior to infection with 1.5 μg DNA and Fugene 6 transfection reagent (Promega). Knockdown of ARNO was performed using the ARNO-specific small interfering RNAs (siRNAs) Hs_PSCD2_2 SI00061292, Hs_PSCD2_3 SI00061299, Hs_PSCD2_6 SI03050894, and Hs_PSCD2_7 SI03072629 or AllStars negative-control siRNA SI03650318 (Qiagen) and HiPerFect transfection reagent (Qiagen).

Infection of cells. Bacteria (optical density at 600 nm [OD_{600}], 0.3 to 0.4) were added to cell monolayers at a multiplicity of infection (MOI) of 200 to 300:1 (bacteria to cell) or, for strains containing pIL22, at an MOI of 10:1. Cells were centrifuged at 700 × *g* for 10 min and then incubated at 37°C for a specified additional period of time. SecinH3 (2.5 μM; Calbiochem) or LY294002 (50 μM; Cell Signaling; catalog no. 9901S) was added immediately prior to addition of bacteria. Infected monolayers were washed, fixed in 3.7% paraformaldehyde for 15 to 20 min, and permeabilized with 1% Triton X-100. Labeling was performed using antibodies to *S. flexneri* 2a lipopolysaccharide (LPS; Gibco) or HA (Covance MMS-101P) or with Myc (Clontech 631206), phalloidin (Invitrogen), or DAPI (100 μM; Invitrogen).

Gentamicin protection assay. Cells seeded at 3×10^5 per well of a 6-well dish were infected at an MOI of 0.02:1 (69); incubated at 37°C for 5 or 50 min; washed three times; incubated for an additional 45 or 60 min, respectively, in DMEM containing 50 μg/ml gentamicin to kill extracellular bacteria; and lysed with 0.5 to 1% Triton X-100. Bacteria in cell lysates and in the initial inoculum were determined by plating.

Protein production and secretion. Synthesis and secretion of IpgD were assayed essentially as described previously (70). Proteins were resolved by SDS-PAGE and probed with IpgD (gift of A. Phalipon [24]) or DnaK (StressGen) antibody.

Pulldown assay. GTP-bound ARF6 in infected monolayers was measured per the manufacturer's instructions (Cytoskeleton, Inc.). Briefly, cells were infected at an MOI of 300:1 (as described above), followed by incubation for an additional 10 or 30 min, lysis on ice, and harvesting and snap-freezing of the lysate. Two hundred fifty micrograms of each lysate was incubated with beads covalently conjugated to the ARF6 binding domain of GGA3 for 1 h at 4°C. Beads were washed and recovered. Bound ARF6 was resolved by SDS-PAGE and analyzed using ARF6 antibody (gift of J. Donaldson). Other antibodies used were phosphor-Akt S473 and pan-Akt (Cell Signaling) and ARNO (Abcam ab56510).

Microscopy and data analysis. Microscopy was performed on a Nikon Eclipse TE300 or TE2000 microscope with Chroma Technology filters. For all sets of experiments, three or more independent experiments were performed. Samples were blinded. At least 10 infected cells were analyzed for each condition. A bacterium was counted as entering the cell if it was found associated with a membrane ruffle, determined by actin staining and phase microscopy, and as potentially undergoing bacterial entry if it was adherent and/or within a membrane ruffle. A cell was counted as infected if at least one bacterium was entering or present within the cell. The significance of differences between two-way comparisons was determined by paired *t* test. The significance of differences among multiple sets of data was determined by one-way analysis of variance (ANOVA) followed by a *post hoc* Tukey comparison.

SUPPLEMENTAL MATERIAL

Supplemental material for this article may be found at http://mbio.asm.org/lookup/suppl/doi:10.1128/mBio.02584-14/-/DCSupplemental.

Figure S1, TIF file, 0.6 MB.
Figure S2, TIF file, 2.7 MB.
Figure S3, TIF file, 0.2 MB.
Figure S4, TIF file, 1.4 MB.
Figure S5, TIF file, 0.3 MB.
Figure S6, TIF file, 0.2 MB.

ACKNOWLEDGMENTS

We acknowledge C. R. Yi and S. Y. Lee for bacterial strain construction and B. B. Herrera for technical support. We thank W. Annaert, J. G. Donaldson, L. C. Santy, R. R. Isberg, A. Phalipon, H. Ploegh, and C. F. Lesser for providing reagents; V. W. Hsu for helpful advice; and J. R. Mayers for critical reading of the manuscript.

This work was supported by Public Health Service grant R01AI081724 (to M.B.G.), trainee support on T32GM007753 (to A.C.G.-M.), and T32AI007061 (to K.A.M. and B.C.R.) from the National Institutes of Health.

REFERENCES

1. **Hale TL**. 1991. Genetic basis of virulence in Shigella species. Microbiol Rev **55:**206–224.
2. **Sansonetti PJ, Kopecko DJ, Formal SB**. 1982. Involvement of a plasmid in the invasive ability of Shigella flexneri. Infect Immun **35:**852–860.
3. **Sasakawa C, Kamata K, Sakai T, Makino S, Yamada M, Okada N, Yoshikawa M**. 1988. Virulence-associated genetic regions comprising 31 kilobases of the 230-kilobase plasmid in Shigella flexneri 2a. J Bacteriol **170:**2480–2484.
4. **Schroeder GN, Hilbi H**. 2008. Molecular pathogenesis of Shigella spp.: controlling host cell signaling, invasion, and death by type III secretion. Clin Microbiol Rev **21:**134–156. http://dx.doi.org/10.1128/CMR.00032-07.
5. **Tran Van Nhieu G, Ben-Ze'ev A, Sansonetti PJ**. 1997. Modulation of bacterial entry into epithelial cells by association between vinculin and the Shigella IpaA invasin. EMBO J **16:**2717–2729. http://dx.doi.org/10.1093/emboj/16.10.2717.
6. **Mounier J, Laurent V, Hall A, Fort P, Carlier MF, Sansonetti PJ, Egile C**. 1999. Rho family GTPases control entry of *Shigella flexneri* into epithelial cells but not intracellular motility. J Cell Sci **112:**2069–2080.
7. **Handa Y, Suzuki M, Ohya K, Iwai H, Ishijima N, Koleske AJ, Fukui Y, Sasakawa C**. 2007. Shigella IpgB1 promotes bacterial entry through the ELMO-Dock180 machinery. Nat Cell Biol **9:**121–128. http://dx.doi.org/10.1038/ncb1526.
8. **Hachani A, Biskri L, Rossi G, Marty A, Ménard R, Sansonetti P, Parsot C, Van Nhieu GT, Bernardini ML, Allaoui A**. 2008. IpgB1 and IpgB2, two homologous effectors secreted via the Mxi-Spa type III secretion apparatus, cooperate to mediate polarized cell invasion and inflammatory potential of Shigella flexneri. Microbes Infect **10:**260–268. http://dx.doi.org/10.1016/j.micinf.2007.11.011.
9. **Takai Y, Sasaki T, Matozaki T**. 2001. Small GTP-binding proteins. Physiol Rev **81:**153–208. http://dx.doi.org/10.1016/S0074-7696(08)61861-6.
10. **Baxt LA, Garza-Mayers AC, Goldberg MB**. 2013. Bacterial subversion of host innate immune pathways. Science **340:**697–701. http://dx.doi.org/10.1126/science.1235771.
11. **D'Souza-Schorey C, Chavrier P**. 2006. ARF proteins: roles in membrane traffic and beyond. Nat Rev Mol Cell Biol **7:**347–358. http://dx.doi.org/10.1038/nrm1910.
12. **Donaldson JG, Jackson CL**. 2011. ARF family G proteins and their regulators: roles in membrane transport, development and disease. Nat Rev Mol Cell Biol **12:**362–375. http://dx.doi.org/10.1038/nrm3117.
13. **Honda A, Nogami M, Yokozeki T, Yamazaki M, Nakamura H, Watanabe H, Kawamoto K, Nakayama K, Morris AJ, Frohman MA, Kanaho Y**. 1999. Phosphatidylinositol 4-phosphate 5-kinase alpha is a downstream effector of the small G protein ARF6 in membrane ruffle formation. Cell **99:**521–532. http://dx.doi.org/10.1016/S0092-8674(00)81540-8.
14. **D'Souza-Schorey C, Li G, Colombo MI, Stahl PD**. 1995. A regulatory role for ARF6 in receptor-mediated endocytosis. Science **267:**1175–1178. http://dx.doi.org/10.1126/science.7855600.
15. **Peters PJ, Hsu VW, Ooi CE, Finazzi D, Teal SB, Oorschot V, Donaldson JG, Klausner RD**. 1995. Overexpression of wild-type and mutant ARF1 and ARF6: distinct perturbations of nonoverlapping membrane compartments. J Cell Biol **128:**1003–1017. http://dx.doi.org/10.1083/jcb.128.6.1003.
16. **Radhakrishna H, Al-Awar O, Khachikian Z, Donaldson JG**. 1999. ARF6 requirement for Rac ruffling suggests a role for membrane trafficking in cortical actin rearrangements. J Cell Sci **112:**855–866.
17. **Santy LC, Ravichandran KS, Casanova JE**. 2005. The DOCK180/Elmo complex couples ARNO-mediated Arf6 activation to the downstream activation of Rac1. Curr Biol **15:**1749–1754. http://dx.doi.org/10.1016/j.cub.2005.08.052.
18. **Humphreys D, Davidson A, Hume PJ, Koronakis V**. 2012. Salmonella virulence effector SopE and host GEF ARNO cooperate to recruit and activate WAVE to trigger bacterial invasion. Cell Host Microbe **11:**129–139. http://dx.doi.org/10.1016/j.chom.2012.01.006.
19. **Humphreys D, Davidson AC, Hume PJ, Makin LE, Koronakis V**. 2013. Arf6 coordinates actin assembly through the WAVE complex, a mechanism usurped by Salmonella to invade host cells. Proc Natl Acad Sci U S A **110:**16880–16885. http://dx.doi.org/10.1073/pnas.1311680110.
20. **Balañá ME, Niedergang F, Subtil A, Alcover A, Chavrier P, Dautry-Varsat A**. 2005. ARF6 GTPase controls bacterial invasion by actin remodelling. J Cell Sci **118:**2201–2210. http://dx.doi.org/10.1242/jcs.02351.
21. **Wong KW, Isberg RR**. 2003. Arf6 and phosphoinositol-4-phosphate-5-kinase activities permit bypass of the Rac1 requirement for beta1 integrin-mediated bacterial uptake. J Exp Med **198:**603–614. http://dx.doi.org/10.1084/jem.20021363.
22. **Selyunin AS, Sutton SE, Weigele BA, Reddick LE, Orchard RC, Bresson SM, Tomchick DR, Alto NM**. 2011. The assembly of a GTPase-kinase signalling complex by a bacterial catalytic scaffold. Nature **469:**107–111. http://dx.doi.org/10.1038/nature09593.
23. **Le Gall T, Mavris M, Martino MC, Bernardini ML, Denamur E, Parsot C**. 2005. Analysis of virulence plasmid gene expression defines three classes of effectors in the type III secretion system of Shigella flexneri. Microbiology **151:**951–962. http://dx.doi.org/10.1099/mic.0.27639-0.
24. **Niebuhr K, Giuriato S, Pedron T, Philpott DJ, Gaits F, Sable J, Sheetz MP, Parsot C, Sansonetti PJ, Payrastre B**. 2002. Conversion of PtdIns(4,5)P(2) into PtdIns(5)P by the S. flexneri effector IpgD reorganizes host cell morphology. EMBO J **21:**5069–5078. http://dx.doi.org/10.1093/emboj/cdf522.
25. **Niebuhr K, Jouihri N, Allaoui A, Gounon P, Sansonetti PJ, Parsot C**. 2000. IpgD, a protein secreted by the type III secretion machinery of Shigella flexneri, is chaperoned by IpgE and implicated in entry focus formation. Mol Microbiol **38:**8–19. http://dx.doi.org/10.1046/j.1365-2958.2000.02041.x.
26. **Sannerud R, Declerck I, Peric A, Raemaekers T, Menendez G, Zhou L, Veerle B, Coen K, Munck S, De Strooper B, Schiavo G, Annaert W**. 2011. ADP ribosylation factor 6 (ARF6) controls amyloid precursor protein (APP) processing by mediating the endosomal sorting of BACE1. Proc Natl Acad Sci U S A **108:**E559–E568. http://dx.doi.org/10.1073/pnas.1100745108.
27. **Sansonetti PJ, Ryter A, Clerc P, Maurelli AT, Mounier J**. 1986. Multiplication of *Shigella flexneri* within HeLa cells: lysis of the phagocytic vacuole and plasmid-mediated contact hemolysis. Infect Immun **51:**461–469.
28. **Ray K, Bobard A, Danckaert A, Paz-Haftel I, Clair C, Ehsani S, Tang C, Sansonetti P, Tran GV, Enninga J**. 2010. Tracking the dynamic interplay between bacterial and host factors during pathogen-induced vacuole rupture in real time. Cell Microbiol **12:**545–556. http://dx.doi.org/10.1111/j.1462-5822.2010.01428.x.
29. **Santy LC, Casanova JE**. 2001. Activation of ARF6 by ARNO stimulates epithelial cell migration through downstream activation of both Rac1 and phospholipase D. J Cell Biol **154:**599–610. http://dx.doi.org/10.1083/jcb.200104019.
30. **Antonny B, Beraud-Dufour S, Chardin P, Chabre M**. 1997. N-terminal hydrophobic residues of the G-protein ADP-ribosylation factor-1 insert into membrane phospholipids upon GDP to GTP exchange. Biochemistry **36:**4675–4684. http://dx.doi.org/10.1021/bi962252b.
31. **Gaschet J, Hsu VW**. 1999. Distribution of ARF6 between membrane and cytosol is regulated by its GTPase cycle. J Biol Chem **274:**20040–20045. http://dx.doi.org/10.1074/jbc.274.28.20040.
32. **Yang CZ, Heimberg H, D'Souza-Schorey C, Mueckler MM, Stahl PD**. 1998. Subcellular distribution and differential expression of endogenous

ADP-ribosylation factor 6 in mammalian cells. J Biol Chem **273:** 4006–4011. http://dx.doi.org/10.1074/jbc.273.7.4006.
33. **Huang Z, Sutton SE, Wallenfang AJ, Orchard RC, Wu X, Feng Y, Chai J, Alto NM.** 2009. Structural insights into host GTPase isoform selection by a family of bacterial GEF mimics. Nat Struct Mol Biol **16:**853–860. http://dx.doi.org/10.1038/nsmb.1647.
34. **Alto NM, Shao F, Lazar CS, Brost RL, Chua G, Mattoo S, McMahon SA, Ghosh P, Hughes TR, Boone C, Dixon JE.** 2006. Identification of a bacterial type III effector family with G protein mimicry functions. Cell **124:**133–145. http://dx.doi.org/10.1016/j.cell.2005.10.031.
35. **Lu R, Goldberg MB.** 2010. Bacterial exploitation of host cell signaling. Sci Transl Med **2:**51ps48. http://dx.doi.org/10.1126/scitranslmed.3001612.
36. **Burnaevskiy N, Fox TG, Plymire DA, Ertelt JM, Weigele BA, Selyunin AS, Way SS, Patrie SM, Alto NM.** 2013. Proteolytic elimination of N-myristoyl modifications by the Shigella virulence factor IpaJ. Nature **496:**106–109. http://dx.doi.org/10.1038/nature12004.
37. **Langille SE, Patki V, Klarlund JK, Buxton JM, Holik JJ, Chawla A, Corvera S, Czech MP.** 1999. ADP-ribosylation factor 6 as a target of guanine nucleotide exchange factor GRP1. J Biol Chem **274:**27099–27104. http://dx.doi.org/10.1074/jbc.274.38.27099.
38. **Frank S, Upender S, Hansen SH, Casanova JE.** 1998. ARNO is a guanine nucleotide exchange factor for ADP-ribosylation factor 6. J Biol Chem **273:**23–27. http://dx.doi.org/10.1074/jbc.273.1.23.
39. **Myers KR, Wang G, Sheng Y, Conger KK, Casanova JE, Zhu JJ.** 2012. Arf6-GEF BRAG1 regulates JNK-mediated synaptic removal of GluA1-containing AMPA receptors: a new mechanism for nonsyndromic X-linked mental disorder. J Neurosci **32:**11716–11726. http://dx.doi.org/10.1523/JNEUROSCI.1942-12.2012.
40. **Ikenouchi J, Umeda M.** 2010. FRMD4A regulates epithelial polarity by connecting Arf6 activation with the PAR complex. Proc Natl Acad Sci U S A **107:**748–753. http://dx.doi.org/10.1073/pnas.0908423107.
41. **Sabe H, Hashimoto S, Morishige M, Ogawa E, Hashimoto A, Nam JM, Miura K, Yano H, Onodera Y.** 2009. The EGFR-GEP100-Arf6-AMAP1 signaling pathway specific to breast cancer invasion and metastasis. Traffic **10:**982–993. http://dx.doi.org/10.1111/j.1600-0854.2009.00917.x.
42. **Hafner M, Schmitz A, Grüne I, Srivatsan SG, Paul B, Kolanus W, Quast T, Kremmer E, Bauer I, Famulok M.** 2006. Inhibition of cytohesins by SecinH3 leads to hepatic insulin resistance. Nature **444:**941–944. http://dx.doi.org/10.1038/nature05415.
43. **Liu L, Pohajdak B.** 1992. Cloning and sequencing of a human cDNA from cytolytic NK/T cells with homology to yeast SEC7. Biochim Biophys Acta **1132:**75–78. http://dx.doi.org/10.1016/0167-4781(92)90055-5.
44. **Li J, Malaby AW, Famulok M, Sabe H, Lambright DG, Hsu VW.** 2012. Grp1 plays a key role in linking insulin signaling to glut4 recycling. Dev Cell **22:**1286–1298. http://dx.doi.org/10.1016/j.devcel.2012.03.004.
45. **Klarlund JK, Tsiaras W, Holik JJ, Chawla A, Czech MP.** 2000. Distinct polyphosphoinositide binding selectivities for pleckstrin homology domains of GRP1-like proteins based on diglycine versus triglycine motifs. J Biol Chem **275:**32816–32821. http://dx.doi.org/10.1074/jbc.M002435200.
46. **Ogasawara M, Kim SC, Adamik R, Togawa A, Ferrans VJ, Takeda K, Kirby M, Moss J, Vaughan M.** 2000. Similarities in function and gene structure of cytohesin-4 and cytohesin-1, guanine nucleotide-exchange proteins for ADP-ribosylation factors. J Biol Chem **275:**3221–3230. http://dx.doi.org/10.1074/jbc.275.5.3221.
47. **Pendaries C, Tronchère H, Arbibe L, Mounier J, Gozani O, Cantley L, Fry MJ, Gaits-Iacovoni F, Sansonetti PJ, Payrastre B.** 2006. PtdIns5P activates the host cell PI3-kinase/Akt pathway during *Shigella flexneri* infection. EMBO J. **25:**1024–1034. http://dx.doi.org/10.1038/sj.emboj.7601001.
48. **Klarlund JK, Guilherme A, Holik JJ, Virbasius JV, Chawla A, Czech MP.** 1997. Signaling by phosphoinositide-3,4,5-trisphosphate through proteins containing pleckstrin and Sec7 homology domains. Science **275:** 1927–1930. http://dx.doi.org/10.1126/science.275.5308.1927.
49. **Venkateswarlu K, Oatey PB, Tavaré JM, Cullen PJ.** 1998. Insulin-dependent translocation of ARNO to the plasma membrane of adipocytes requires phosphatidylinositol 3-kinase. Curr Biol **8:**463–466. http://dx.doi.org/10.1016/S0960-9822(98)70181-2.
50. **Nagel W, Schilcher P, Zeitlmann L, Kolanus W.** 1998. The PH domain and the polybasic c domain of cytohesin-1 cooperate specifically in plasma membrane association and cellular function. Mol Biol Cell **9:**1981–1994. http://dx.doi.org/10.1091/mbc.9.8.1981.
51. **Manna D, Albanese A, Park WS, Cho W.** 2007. Mechanistic basis of differential cellular responses of phosphatidylinositol 3,4-bisphosphate- and phosphatidylinositol 3,4,5-trisphosphate-binding pleckstrin homology domains. J Biol Chem **282:**32093–32105. http://dx.doi.org/10.1074/jbc.M703517200.
52. **Brandman O, Meyer T.** 2008. Feedback loops shape cellular signals in space and time. Science **322:**390–395. http://dx.doi.org/10.1126/science.1160617.
53. **Feng S, Knödler A, Ren J, Zhang J, Zhang X, Hong Y, Huang S, Peränen J, Guo W.** 2012. A Rab8 guanine nucleotide exchange factor-effector interaction network regulates primary ciliogenesis. J Biol Chem **287:** 15602–15609. http://dx.doi.org/10.1074/jbc.M111.333245.
54. **Ortiz D, Medkova M, Walch-Solimena C, Novick P.** 2002. Ypt32 recruits the Sec4p guanine nucleotide exchange factor, Sec2p, to secretory vesicles; evidence for a Rab cascade in yeast. J Cell Biol **157:**1005–1015. http://dx.doi.org/10.1083/jcb.200201003.
55. **Stalder D, Barelli H, Gautier R, Macia E, Jackson CL, Antonny B.** 2011. Kinetic studies of the Arf activator Arno on model membranes in the presence of Arf effectors suggest control by a positive feedback loop. J Biol Chem **286:**3873–3883. http://dx.doi.org/10.1074/jbc.M110.145532.
56. **Richardson BC, McDonold CM, Fromme JC.** 2012. The Sec7 Arf-GEF is recruited to the trans-Golgi network by positive feedback. Dev Cell **22:** 799–810. http://dx.doi.org/10.1016/j.devcel.2012.02.006.
57. **Cohen LA, Honda A, Varnai P, Brown FD, Balla T, Donaldson JG.** 2007. Active Arf6 recruits ARNO/cytohesin GEFs to the PM by binding their PH domains. Mol Biol Cell **18:**2244–2253. http://dx.doi.org/10.1091/mbc.E06-11-0998.
58. **Macia E, Paris S, Chabre M.** 2000. Binding of the PH and polybasic C-terminal domains of ARNO to phosphoinositides and to acidic lipids. Biochemistry **39:**5893–5901. http://dx.doi.org/10.1021/bi992795w.
59. **Auger KR, Cantley LC.** 1991. Novel polyphosphoinositides in cell growth and activation. Cancer Cells **3:**263–270.
60. **DiNitto JP, Cronin TC, Lambright DG.** 2003. Membrane recognition and targeting by lipid-binding domains. Sci STKE **2003:**re16. http://dx.doi.org/10.1126/stke.2132003re16.
61. **Cronin TC, DiNitto JP, Czech MP, Lambright DG.** 2004. Structural determinants of phosphoinositide selectivity in splice variants of Grp1 family PH domains. EMBO J **23:**3711–3720. http://dx.doi.org/10.1038/sj.emboj.7600388.
62. **Allaoui A, Ménard R, Sansonetti PJ, Parsot C.** 1993. Characterization of the *Shigella flexneri* ipgD and ipgF genes, which are located in the proximal part of the mxi locus. Infect Immun **61:**1707–1714.
63. **Mellouk N, Weiner A, Aulner N, Schmitt C, Elbaum M, Shorte SL, Danckaert A, Enninga J.** 2014. Shigella subverts the host recycling compartment to rupture its vacuole. Cell Host Microbe **16:**517–530. http://dx.doi.org/10.1016/j.chom.2014.09.005.
64. **Ramel D, Lagarrigue F, Pons V, Mounier J, Dupuis-Coronas S, Chicanne G, Sansonetti PJ, Gaits-Iacovoni F, Tronchère H, Payrastre B.** 2011. *Shigella flexneri* infection generates the lipid PI5P to alter endocytosis and prevent termination of EGFR signaling. Sci Signal **4:**ra61. http://dx.doi.org/10.1126/scisignal.2001619.
65. **Konradt C, Frigimelica E, Nothelfer K, Puhar A, Salgado-Pabon W, di Bartolo V, Scott-Algara D, Rodrigues CD, Sansonetti PJ, Phalipon A.** 2011. The *Shigella flexneri* type three secretion system effector IpgD inhibits T cell migration by manipulating host phosphoinositide metabolism. Cell Host Microbe **9:**263–272. http://dx.doi.org/10.1016/j.chom.2011.03.010.
66. **Puhar A, Tronchère H, Payrastre B, Nhieu GT, Sansonetti PJ.** 2013. A Shigella effector dampens inflammation by regulating epithelial release of danger signal ATP through production of the lipid mediator PtdIns5P. Immunity **39:**1121–1131. http://dx.doi.org/10.1016/j.immuni.2013.11.013.
67. **Viaud J, Lagarrigue F, Ramel D, Allart S, Chicanne G, Ceccato L, Courilleau D, Xuereb JM, Pertz O, Payrastre B, Gaits-Iacovoni F.** 2014. Phosphatidylinositol 5-phosphate regulates invasion through binding and activation of Tiam1. Nat Commun **5:**4080. http://dx.doi.org/10.1038/ncomms5080.
68. **Labrec EH, Schneider H, Magnani TJ, Formal SB.** 1964. Epithelial cell penetration as an essential step in the pathogenesis of bacillary dysentery. J. Bacteriol. **88:**1503–1518.

69. **Isberg RR, Falkow S.** 1985. A single genetic locus encoded by *Yersinia pseudotuberculosis* permits invasion of cultured animal cells by *Escherichia coli* K-12. Nature **317:**262–264. http://dx.doi.org/10.1038/317262a0.
70. **Parsot C, Ménard R, Gounon P, Sansonetti PJ.** 1995. Enhanced secretion through the *Shigella flexneri* Mxi-Spa translocon leads to assembly of extracellular proteins into macromolecular structures. Mol Microbiol **16:** 291–300. http://dx.doi.org/10.1111/j.1365-2958.1995.tb02301.x.
71. **Marquart ME, Picking WL, Picking WD.** 1996. Soluble invasion plasmid antigen C (IpaC) from *Shigella flexneri* elicits epithelial cell responses related to pathogen invasion. Infect Immun **64:**4182–4187.
72. **Labigne-Roussel AF, Lark D, Schoolnik G, Falkow S.** 1984. Cloning and expression of an afimbrial adhesin (AFA-I) responsible for P blood group-independent, mannose-resistant hemagglutination from a pyelonephritic *Escherichia coli* strain. Infect Immun **46:**251–259.